

SAR Calculations of Novel Textile Dual-Layer UWB Lotus Antenna for Astronauts Spacesuit

Mohamed I. Ahmed^{1,*}, Mai F. Ahmed², and Abd-El A. Shaalan²

Abstract—A novel dual-layer ultra-wideband lotus-wearable antenna is presented in this paper for integration on astronaut's flight jacket to monitor the vital signs of astronauts. The proposed antenna is designed and fabricated on a leather material as a substrate to operate over a frequency band (2–12 GHz). The dielectric constant $\epsilon_r = 1.79$ and loss tangent $\tan \delta = 0.042$ of the leather material are measured by using two different methods. The proposed antenna has three-strip lines in the 2nd layer for performance enhancement. The stretching effect of the proposed antenna on its impedance characteristics is studied. Furthermore, SAR calculations are performed in on-body environments to ensure that it operates properly in the nearness of the human body. Finally, the proposed design is simulated by CST simulator version 2016, fabricated using folded copper and measured by Agilent 8719ES VNA. The measured results agree well with the simulated ones.

1. INTRODUCTION

Ultra-wideband (UWB) antennas have received increasing attention in recent years. These antennas are very attractive in modern and future wireless communication systems such as handheld devices and body-worn communication systems. The main advantage of UWB antennas is that the use of one UWB antenna is more efficient than the use of multiple narrow-band antennas, which can effectively reduce the number of antennas [1–3].

A lot of applications include smart cloths with wireless communication devices for sports, astronaut's space suit, military suit, fire fighter's uniform and emergency worker's uniform [4–6]. From an engineer's point of view, antenna is an indispensable part of any wearable wireless technology. This antenna must be flexible, lightweight, compact and low profile, and also at the same time, it should be mechanically efficient with acceptable wide bandwidth and desirable radiation properties [7–9]. In addition, it must be kept in mind that wearable antennas work very close to the human body, so it is very important to study the effects of these antennas on the human body to ensure that the wearable antennas performed well near human body [10, 11]. For this study, specific absorption ratio (SAR) must be calculated, which aids in the quantitative study of power absorption issues to ensure that the SAR value actually satisfies the international safety standards (FCC & ICNIPR). The SAR quantifies the power absorbed per unit mass of tissue [12, 13]. This quantity is defined as

$$SAR = \frac{\sigma |E|^2}{\rho} \quad (1)$$

where σ is the electrical conductivity in Siemens per meter (S/m), ρ the mass density in kilograms per cubic meter (kg/m^3), and E the electric field intensity vector, with magnitude in volts per meter (V/m).

Received 9 January 2017, Accepted 6 March 2018, Scheduled 26 March 2018

* Corresponding author: Mohamed Ismail Ahmed (miahmed@eri.sci.eg).

¹ Microstrip Department, Electronics Research Institute, Giza, Egypt. ² Department of Electrical & Electronics Engineering, Faculty of Engineering, Zagazig University, Zagazig, Egypt.

In this paper, a novel dual-layer UWB lotus wearable antenna with three strip lines is simulated and fabricated for integrating into a flight jacket of an astronaut to monitor the vital signs of astronauts constantly. A leather flexible textile material is used as substrate material. This antenna is designed to operate over a frequency band (2–12 GHz). In addition, this lotus wearable antenna may be exposed to stretching due to pressure difference inside and outside the spacesuit. Therefore, the antenna performance characteristics under the stretching conditions are also investigated.

2. MEASUREMENT OF DIELECTRIC CHARACTERISTICS OF LEATHER TEXTILE SUBSTRATES

In order to design a microstrip wearable antenna on textile surface, the dielectric characteristics (dielectric constant ε and loss tangent $\tan \delta$) of the substrate should be known. For this purpose the dielectric constant and loss tangent of the leather substrate must be measured. A leather textile material is chosen because it is more flexible to place within clothing, and it has high water resistance [14]. In this paper the dielectric constant and loss tangent for leather material are measured by using two different methods. The first is a microstrip ring resonator method. In this method, a ring resonator model consists of a ring and two feed lines pasted on the top side of the leather substrate, and the ground plane occupies the bottom side of the leather substrate. A small gap Δ is also included between the ring and each feed line [15, 16]. The fabricated ring resonator model is shown in Fig. 1(a). By measuring S_{21} for this model, shown in Fig. 1(b), the peak in the S_{21} is recorded around each resonance and mentioned in Table 1. The n^{th} resonance occurs at [17]:

$$f_n = \frac{nc}{2\pi r \sqrt{\varepsilon_{\text{eff}}(f)}} \quad (2)$$

where r is the mean radius, c the speed of light in a vacuum, and $\varepsilon_{\text{eff}}(f)$ the frequency dependent effective dielectric constant.

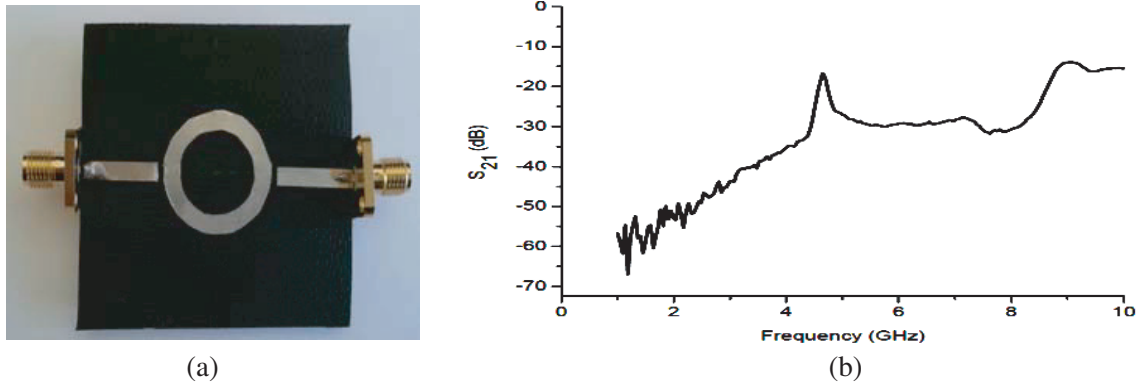


Figure 1. Fabricated ring resonator: (a) fabricated geometry, and (b) measured S_{21} with the frequency.

Table 1. The results of ring resonator method for characterization of leather textile substrate.

Substrate Material	Mode	Resonant Frequency (GHz)	S_{21} (dB)	dielectric constant (ε_r)	loss tangent ($\tan \delta$)
Leather	$n = 1$	4.2	-16.68	1.788	0.041
	$n = 2$	8.81	-13.91	1.72	0.0398

The insertion loss (S_{21} (dB)) is also introduced as [18],

$$IL = 20 \log \left(1 - \frac{Q_L}{Q_u} \right) \quad (3)$$

where Q_L is the loaded quality factor, and Q_u is the unloaded quality factor.

(Hint: if Q_L and Q_U are similar, it means that this material is very lossy, so it must be $Q_u \gg Q_L$ to avoid excessive losses).

Also, the loaded quality factor can be measured from S_{21} curve as [18],

$$Q_L = \frac{f_0}{\Delta f} \quad (4)$$

where f is the resonance frequency, and Δf is the difference between high frequency and low frequency around f ($\Delta f = f_h - f_l$).

To calculate the loss tangent of any material, unloaded quality factor (Q_u) must be firstly determined from Eq. (3) and then applied it in Eq. (5) [19],

$$\frac{1}{Q_u} = \frac{1}{Q_c} + \frac{1}{Q_d} \quad (5)$$

where Q_d is the dielectric quality factor, and Q_c is the conduction quality factor.

The conduction quality factor can be calculated by [19],

$$Q_c = h \sqrt{f_0 \mu_0 \pi \sigma_c} \quad (6)$$

where h is the thickness of substrate, f the resonance frequency, μ the permeability of free space, and σ_c the conductivity of conduction walls.

(Hint: the conductivity of copper $\sigma_c = 2.7 \times 10^7$ s/m is a very large value, so according to Eq. (6), $1/Q_c$ is a very small number which may be neglected).

From Eq. (5), the dielectric quality factor (Q_d) can be determined by subtracting the conductor quality factor (Q_c) from the unloaded quality factor (Q_u), and then the loss tangent can be obtained as [19],

$$\tan \delta = \frac{1}{Q_d} \quad (7)$$

The second method is DAK (Dielectric Assessment Kit) equipment [20]. This method is used to confirm the results obtained from the ring resonator method. The thickness of the leather material is measured by using screw gauge. The measured dielectric constant, loss tangent and thickness of the leather substrate are mentioned in Table 2.

Table 2. The characterization results of the leather textile substrate.

Substrate Material	Dielectric constant (ϵ_r)	loss tangent ($\tan \delta$)	Thickness (mm)
Leather	1.79	0.042	1.3

From comparing the obtained results using the two methods, it can be observed that both of them estimate much close values of leather material, but there are some slight differences between them, and this is an inherent thing.

3. ANTENNAS DESIGN AND RESULTS DISCUSSION

A three-dimensional view of the proposed dual-layer UWB lotus wearable antenna with a three strip lines pasted on the leather textile material as the substrate without any metallization is shown in Fig. 2.

In layer 1, a novel lotus patch is fed by a microstrip line that consists of two parts: 50Ω line feed and tapered feed to improve the impedance matching and achieve the best results as shown in Fig. 2(a). In layer II, three microstrip lines are integrated and bounded the proposed antenna for eliminating the surface waves and increasing the bandwidth and efficiency for performance enhancement as shown in Fig. 2(b). Also, the ground plane with a small notch with angle 45° for improving the matching impedance and also with a thin track for reducing the surface wave is pasted on the back side of the bottom substrate as shown in Fig. 2(c). The optimized dimensions are mentioned in Table 3 according to Fig. 2. The fabricated geometry of this antenna is shown in Fig. 3.

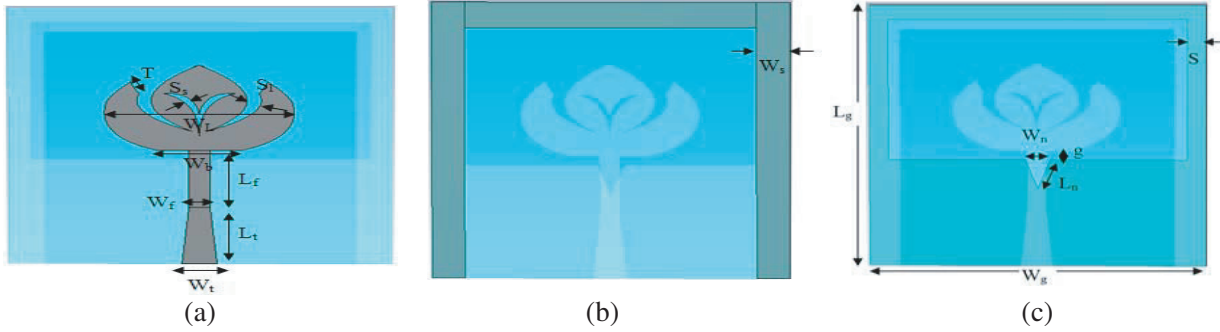


Figure 2. The geometry of lotus antenna, (a) top layer: patch with tapered fed, (b) mid layer: three strip, and (c) bottom layer: ground plane.

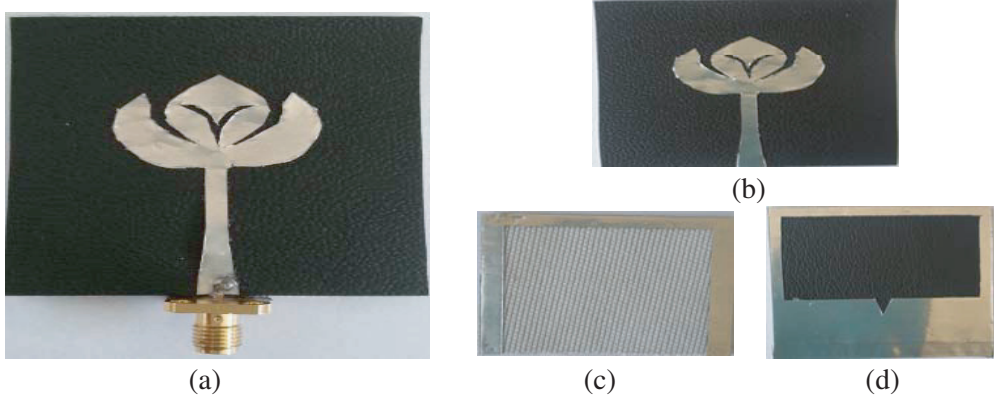


Figure 3. (a) The fabricated geometry of lotus antenna, (b) top layer: patch with tapered fed, (c) mid layer: three strips, and (d) bottom layer: ground plane.

Table 3. The optimized dimensions of the proposed antenna in mm.

W_t	L_t	W_f	L_f	W_b	W_L	S_l	S_s	T	W_n	L_n	W_g	L_g	S	g	W_s
5	12	3	12	12	27	4	2	2.8	4	6.3	54	54	3	2	5

The simulated and measured S_{11} for this antenna are plotted in Fig. 4. From these results, it is found that the measured results agree well with the simulated ones. Also, one notes that in the experimental results a fourth resonance appears at 6 GHz, but it does not appear on the simulated curve. It becomes clear that this resonance comes due to termination of the feeder, which is relatively bulky. In addition, the experimental matching frequency band as in the S_{11} curve has shifted relative to the simulated one by about 0.6 GHz specially the resonance frequencies responsible for the lotus patch part. Obviously, the experimental lotus part has come up with wider tolerance than expected, which causes this large shift due to the bad chipping during manufacturing. These results are obtained on a CST 2016 Simulator. CST MICROWAVE STUDIO is a computer system technology and is a numerical simulator, which uses the finite integration technique (FIT) [21].

The proposed UWB lotus antenna with three stripes is also examined on the spacesuit material. As the main goal is the integration of the lotus antenna on the spacesuit of astronauts, University of North Dakota's NDX-II spacesuit is considered as shown in Fig. 5(a) [22]. We must also keep in mind the effect of antenna bending and crumpling on the performance characteristics. To reduce this influence, the chest part of the spacesuit is considered to be the optimum place to integrate the Lotus antenna. In addition, this antenna is small in size where the smaller textile antenna bends less.

The spacesuit consists of multi-layers; International Space Station EVAs use Ortho-fabric as the

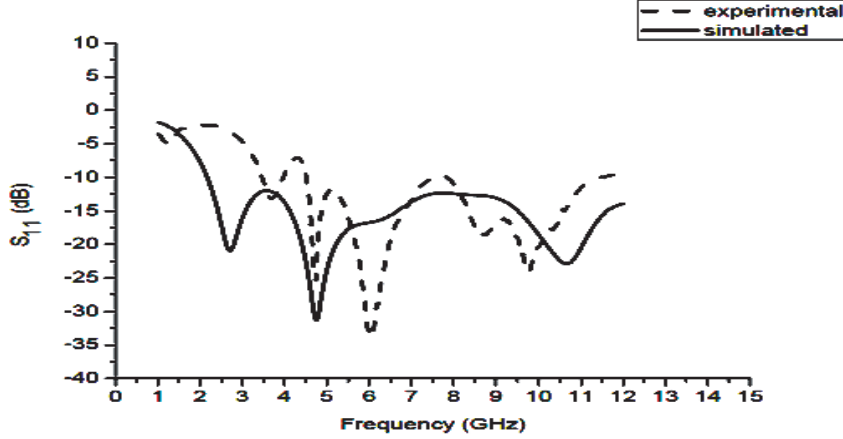


Figure 4. The experimental and simulated S_{11} for the proposed lotus antenna.

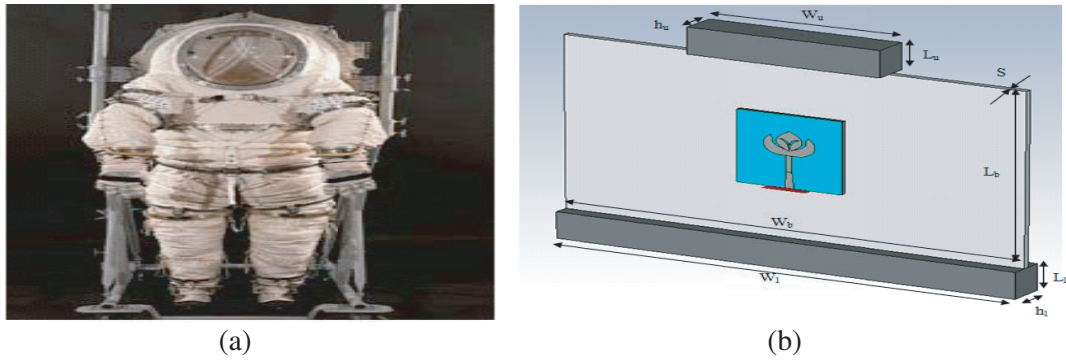


Figure 5. (a) The NDX-II human spaceflight, (b) simulation model of the chest part of the spacesuit with the UWB lotus antenna.

Table 4. The parameters of the spacesuit structure.

Dimensions	W_u	L_u	h_u	W_b	L_b	S	W_l	L_l	h_l
value (mm)	100	20	20	240	130	3.6	240	20	20

outermost layer [23]. Also, the effect of stainless steel rings in the spacesuit is taken into account as shown in Fig. 5(a) [24] and [25]. The simulated structure of the chest part of the spacesuit is shown in Fig. 5(b), and parameters of the spacesuit structure are listed in Table 4.

The simulated S_{11} of the UWB lotus antenna alone and antenna on the spacesuit material are shown in Fig. 6. The current distribution for the proposed lotus antenna is shown in Fig. 7. The simulated E -plane and H -plane radiation patterns of the proposed UWB lotus antenna with and without spacesuit material at four random frequencies 2.45, 5.8, 7, and 9 GHz are shown in Fig. 8 and Fig. 9.

From Fig. 6, it can be noticed that the impedance bandwidth of the antenna on spacesuit is reduced by 0.3 dB compared to the antenna in free space. It can also be noticed from Figs. 8 and 9 that the realized gain of the E -plane and H -plane of the antenna on spacesuit has about 0.5 dB increment compared to the antenna in free space.

4. SAR CALCULATIONS

It is important to make sure that the astronauts are exposed to less electromagnetic waves, and the UWB lotus antenna is safe for astronauts. For these reasons, the specific absorption ratio (SAR) is

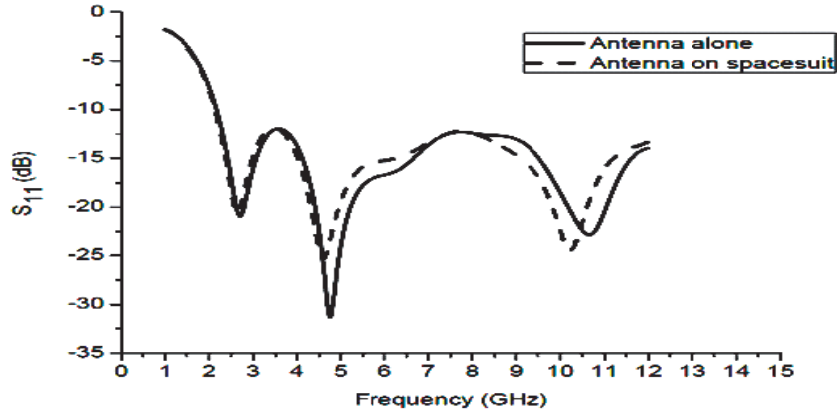


Figure 6. The return loss of the proposed lotus antenna in free space and on spacesuit.

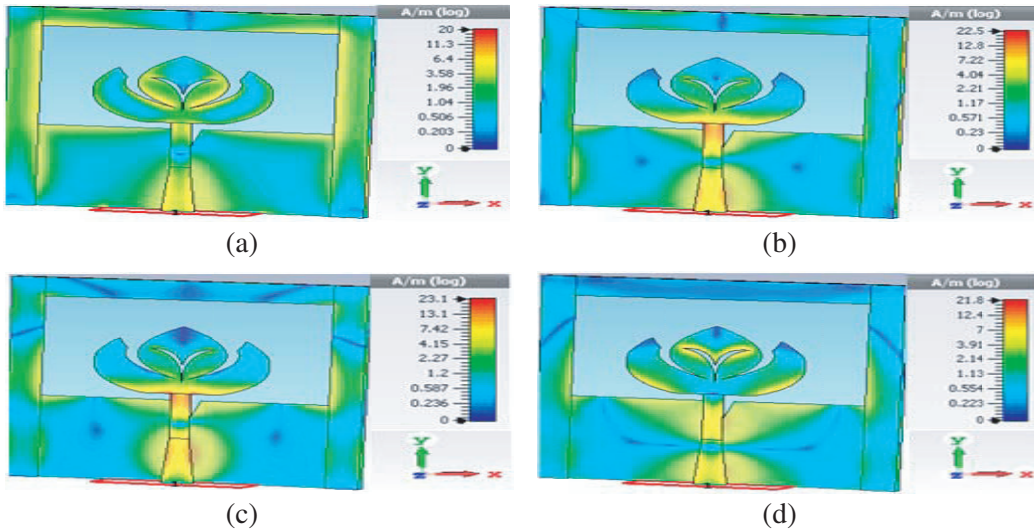


Figure 7. The current distribution for the proposed uwb lotus antenna at four random frequencies, (a) 2.45, (b) 5.8, (c) 7, and (d) 9 GHz.

Table 5. The peak SAR values for the proposed UWB Lotus antenna on spacesuit at a distance 10 mm from antenna by FCC (1g) & ICNIPR (10 g) standards.

Frequency (GHz)	SAR value (w/kg)	
	10 g	1 g
2.45	0.113	0.26
5.8	0.175	0.549
7	0.153	0.505
9	0.352	0.741

studied, which must be satisfies the international safety standards, FCC (SAR < 1.6 W/kg over 1g) and ICNIRP (SAR < 2 W/kg over 10 g). Fig. 10 illustrates the SAR simulation results at four random frequencies 2.45, 5.8, 7, and 9 GHz, and these results are mentioned in Table 5. From these results, note that all the SAR values do not exceed unity.

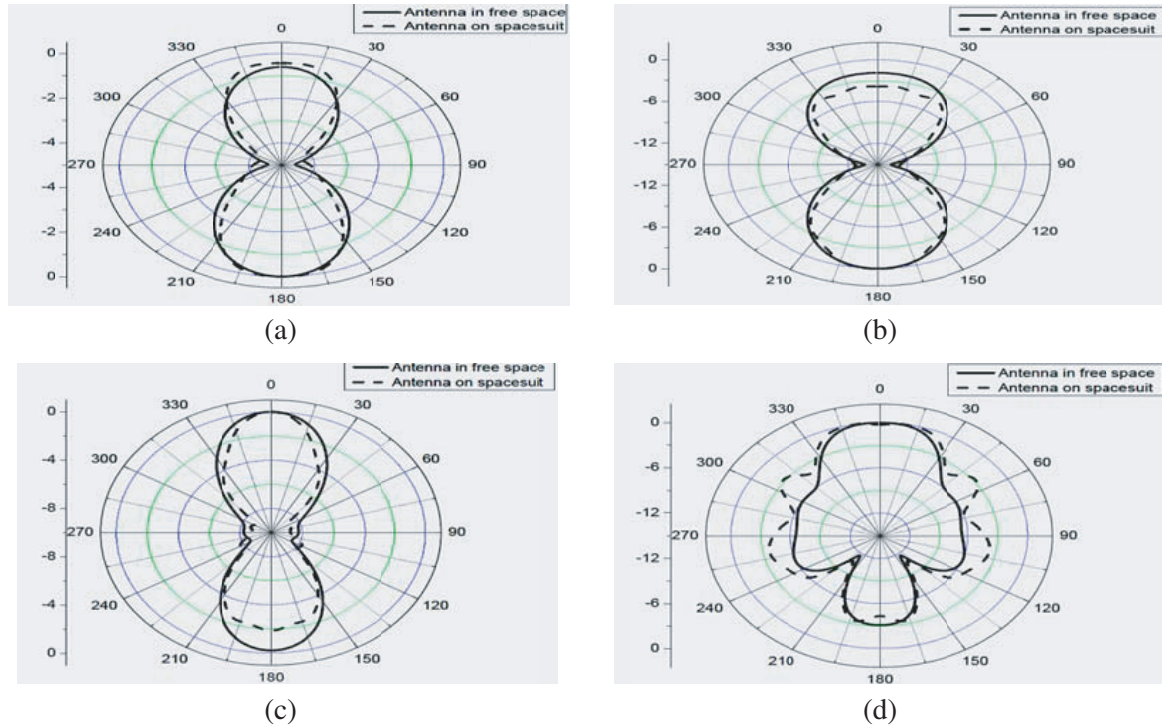


Figure 8. The radiation pattern for the proposed UWB lotus wearable antenna with/without spacesuit material in E -plane ($\varphi = 0^\circ$) at (a) 2.45 GHz, (b) 5.8 GHz, (c) 7 GHz and (d) 9 GHz.

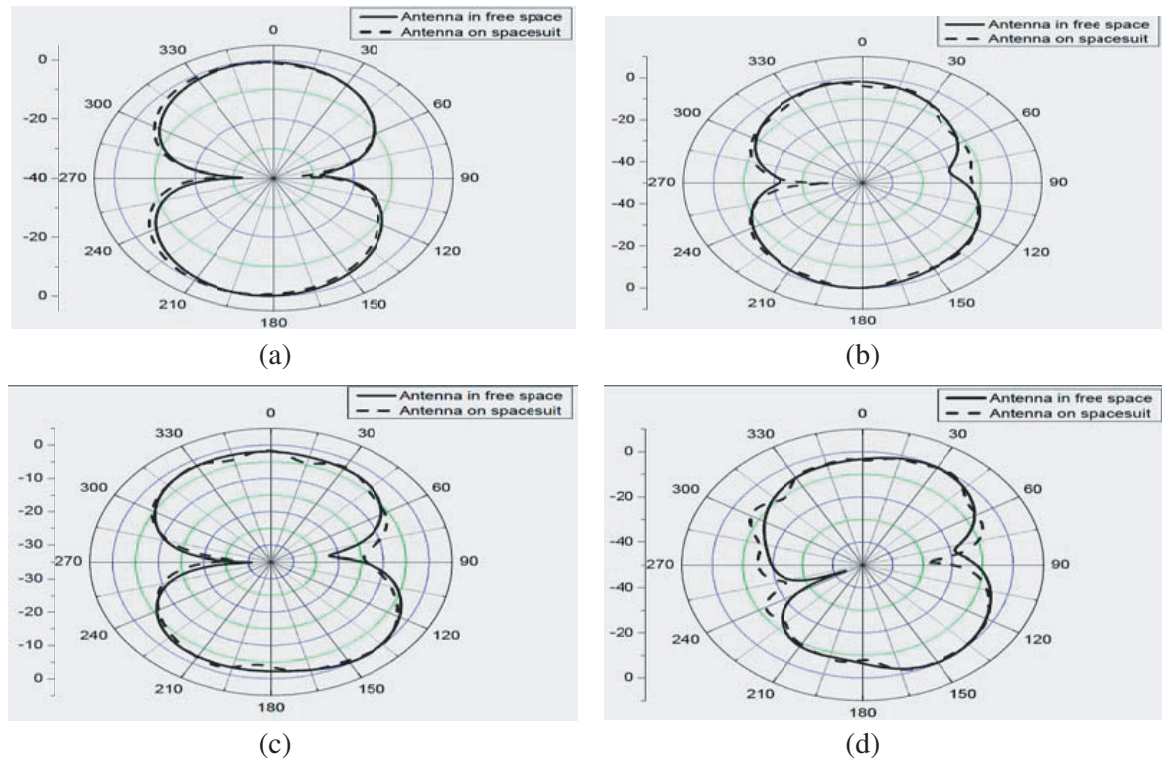


Figure 9. The radiation pattern for the proposed UWB lotus wearable antenna with/without spacesuit material in H -plane ($\varphi = 90^\circ$) at (a) 2.45 GHz, (b) 5.8 GHz, (c) 7 GHz and (d) 9 GHz.

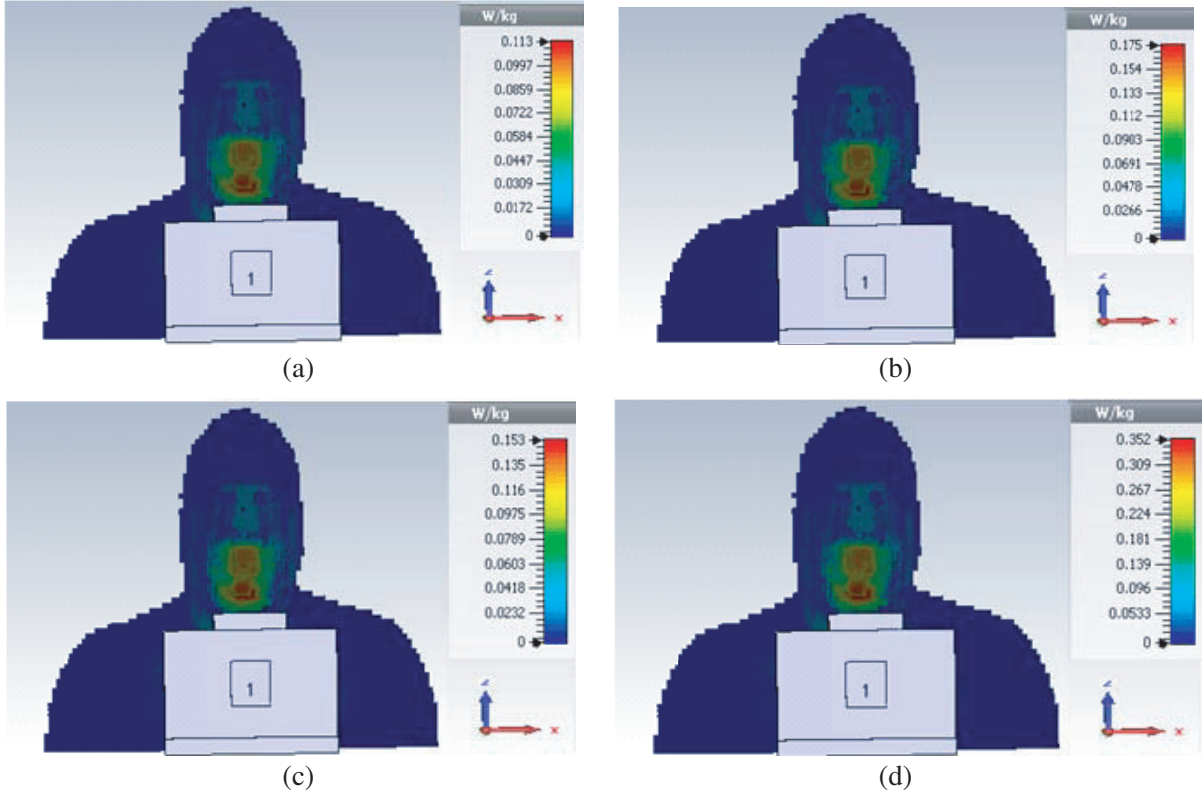


Figure 10. SAR distribution on human voxel model (10 g) in distance 10 mm from Lotus antenna at (a) 2.45 GHz, (b) 5.8 GHz, (c) 7 GHz and (d) 9 GHz.

5. EFFECTS OF ANTENNA STRETCHING ON ITS PERFORMANCE CHARACTERISTICS

As a result of the pressure difference inside and outside the spacesuit, the fabric materials may be exposed to stretch, and because the wearable antenna is made up of textile material, it is also exposed to stretch. Studies have estimated that the expansion rate is estimated at about 3% of its original size [13]. Fig. 11 illustrates the lotus antenna with stretching effect in three cases: length only, width only, and length and width together. The simulated S_{11} for this antenna in different cases of stretching are plotted in Fig. 12.

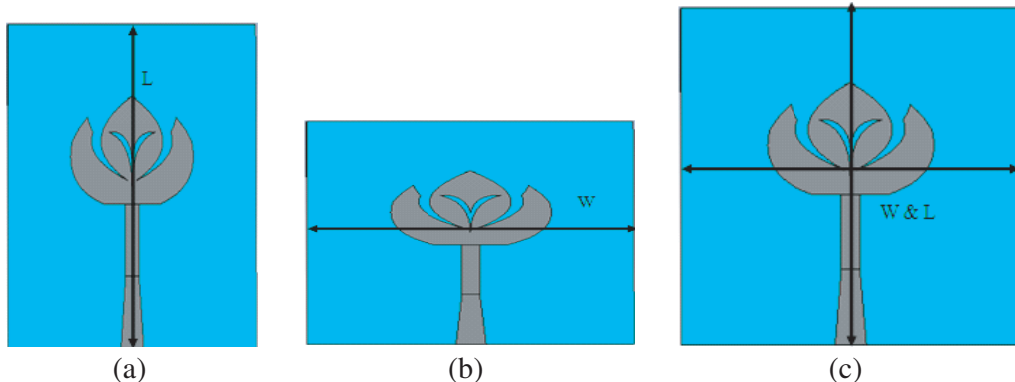


Figure 11. The UWB lotus antenna stretched by: (a) length only, (b) width only, and (c) length & width together.

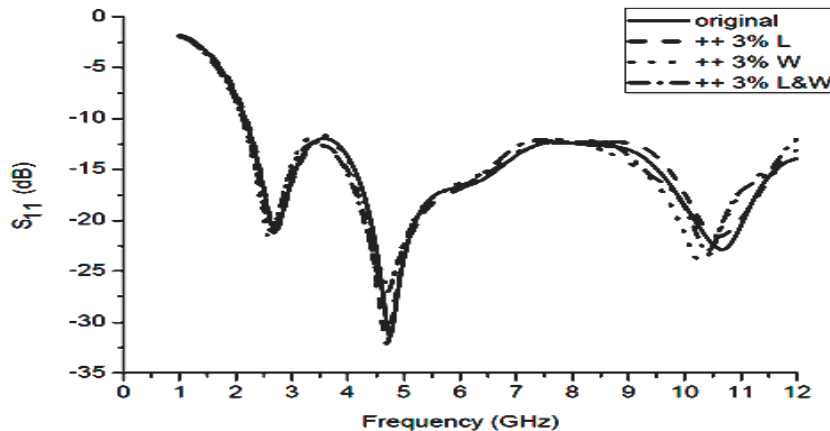


Figure 12. S -parameter comparison for stretching in different cases.

From Fig. 12, it can be noticed that stretching in length does not cause significant changes in the antenna performance. However, when the antenna is stretched in width, the performance drops drastically. Similarly, stretching in both length and width causes a lot of deteriorating effects in the antenna performance.

6. CONCLUSION

A novel dual-layer UWB lotus-wearable antenna is presented in this work. The proposed antenna is simulated and fabricated to operate over a frequency band (2–12 GHz). Leather textile material is used in the proposed antenna as a substrate. The dielectric constant (ϵ_r) and loss tangent ($\tan \delta$) of Leather material are measured by two methods in this paper, microstrip ring resonator method and DAC (Dielectric Assessment Kit) method. The second has been used to confirm the results determined using the first. The proposed antenna is fabricated for integrating into a flight jacket of the astronaut. Exactly, it is allocated on the chest part of the spacesuit to monitor the vital signs of astronauts. Further, the SAR value is considered an important parameter. In our design, the SAR value is very low, thus this antenna operates properly in the nearness of the human body. The effect of antenna stretching on the performance characteristics is also studied.

REFERENCES

1. Kumar, P., "Design of low cross-polarized patch antenna for ultra-wideband applications," *International Journal on Communication Antenna and Propagation*, Vol. 7, No. 4, 265, 2017.
2. Acharya, I. and A. S. Chauhan, "Detailed analysis of a novel fractal monopole antenna for UWB applications with notches for WLAN rejection using two different approaches," *International Journal on Communication Antenna and Propagation*, Vol. 7, No. 3, 233, 2017.
3. Bandi, S., A. Sudhakar, and K. P. Raju, "A microstrip rectangle carpet shaped fractal antenna for UWB applications," *International Journal on Communication Antenna and Propagation*, Vol. 6, No. 2, 111, 2016.
4. Dumanli, S., L. Sayer, E. Mellios, X. Fafoutis, G. Hilton, and I. Craddock, "Off-body antenna wireless performance evaluation in a residential environment," *IEEE Transactions on Antennas and Propagation*, Vol. 65, No. 11, 6076–6084, November 2017.
5. Ahmed, M. I., M. F. Ahmed, and A. A. Shaalan, "CPW ring wearable antenna on leather material for BAN applications," *IEEE International Symposium on Antennas and Propagation and USNC-URSI Radio Science Meeting*, San Diego, California, USA, July 2017.

6. Jiang, Z. H., M. D. Gregory, and D. H. Werner, "Design and experimental investigation of a compact circularly polarized integrated filtering antenna for wearable biotelemetric devices," *IEEE Transactions on Biomedical Circuits and Systems*, Vol. 10, No. 2, 328–338, April 2016.
7. Salvado, R., C. Loss, R. Gonçalves, and P. Pinho, "Textile materials for the design of wearable antennas: A survey," *Sensors*, Vol. 12, No. 11, 15841, 2012.
8. Al Amin, A., M. S. Islam, M. A. Masud, N. H. Khan, J. W. A. Zavala, and M. M. U. Islam, "Design and performance analysis of 3.4 GHz rectangular microstrip patch antenna for wireless communication systems," *International Journal on Communication Antenna and Propagation*, Vol. 7, No. 1, 2017.
9. Salonen, P., Y. Rahmat-Samii, M. Schafhth, and M. Kivikoski, "Effect of textile materials on wearable antenna performance: A case study of GPS antennas," *Antennas & Propagation Society International Symposium*, Vol. 1, 459–462, 2004.
10. Kiourti, A., C. Lee, and J. L. Volakis, "Fabrication of textile antennas and circuits with 0.1 mm precision," *IEEE Antennas and Wireless Propagation Letters*, Vol. 15, 151–153, 2015.
11. Dey, S. and N. Saha, "Narrow band and UWB wearable antennas: Design and assessment of the conformal characteristics in terms of impedance matching and radiation properties," *International Journal on Communication Antenna and Propagation*, Vol. 3, No. 1, 42–50, 2013.
12. Ahmed, M. I., E. A. Abdallah, and H. M. Elhennawy, "SAR investigation of novel wearable reduced-coupling microstrip antenna array," *International Journal of Engineering and Technology-IJENS*, Vol. 15, No. 3, 78–87, June 2015.
13. Ahmed, M. I., M. F. Ahmed, and A. A. Shaalan, "SAR calculations of novel wearable fractal antenna on metamaterial cell for search and rescue applications," *Progress In Electromagnetic Research M*, Vol. 53, 99–110, 2017.
14. Mahmud, M. S., F. J. J. Jabri, and B. Mahjabeen, "Compact UWB wearable antenna on leather material for wireless applications," *IEEE International Symposium on Antennas and Propagation and USNC-URSI Radio Science Meeting*, Vol. 9, No. 6, 2191–2192, Orlando, FL, USA, July 2013.
15. Hopkins, R. and C. Free, "Equivalent circuit for the microstrip ring resonator suitable for broadband materials characterization," *IET Microwaves, Antennas & Propagation*, Vol. 2, No. 1, 66–73, February 2008.
16. Ahmed, M. I., M. F. Ahmed, and A. A. Shaalan, "Investigation and comparsion of wearable bluetooth antennas on different textile substrates," *IEEE International Symposium on Antennas and Propagation and USNC-URSI Radio Science Meeting*, 2633–2634, San Diego, California, USA, July 2017.
17. Rashidian, A., M. T. Aligodarz, and D. M. Klymyshyn, "Dielectric characterization of materials using a modified microstrip ring resonator technique," *IEEE Transactions on Dielectrics and Electrical Insulation*, Vol. 19, No. 4, 1392–1399, August 2012.
18. Chew, W. C., "A broad-band annular-ring microstrip antenna," *IEEE Transactions on Antennas and Propagation*, Vol. 30, No. 5, 918–922, September 1982.
19. Pozar, D. M., *Electromagnetic Theory in Microwave Engineering*, 3rd Edition, 2005.
20. <https://www.speag.com/products/dak/dielectric-measurements/>.
21. CST MICROWAVE STUDIO®, help, <http://www.cst.com>.
22. <http://human.space.edu/projects/NDX-2.htm>.
23. Haagenson, T., S. Noghanian, P. d. León, and Y. Chang, "Textile antenna for space suit applications," *IEEE Antenna and Propagation Magazine*, Vol. 15, 2015.
24. Leon, P. D., G. L. Harris, and A. M. Wargetz, "Design, construction, and implementation of an inflatable lunar habitat base with pressurized rover and suit ports," *International Conference on Environmental Systems*, Vail, Colorado, 2013.
25. Gaier, J. R., "Abrasion of candidate spacesuit fabrics by simulated lunar dust," *International Conference on Environmental Systems*, 2009.